セラミックス基盤工学研究センター年報 (2009). Vol. 9, 23-31

総説

Structural Properties and Surface Characteristics on Aluminum Oxide Powders

Takashi Shirai, Hideo Watanabe, Masayoshi Fuji and Minoru Takahashi

Ceramics Research Laboratory, Nagoya Institute of Technology
Hon-machi 3-101-1, Tajimi, Gifu 507-0033, JAPAN

Abstract

α-Al_2O_3 is widely used and studied as high temperature structural material, electronic packaging, corrosion resistance ceramics and translucent ceramics. The surface state of α-Al_2O_3 powders cannot be regarded as α-Al_2O_3 but a hydrated state, and that the nature of this hydrate cannot be considered universal among different α-Al_2O_3, even produced by the same production method. One of these reasons is that water can be incorporated in the α-Al_2O_3 crystal structure resulting in the formation of aluminum hydroxides such as gibbsite. Although much research has shed light on the Al_2O_3-water interface and charging of α-Al_2O_3 surfaces, there is still much that we need to better understand α-Al_2O_3 structural property and surface characteristics. In this paper, general view of crystal-structural properties, manufacturing methods of high purity α-Al_2O_3, and surface characteristics on α-Al_2O_3 powders are introduced.

1. Aluminum Oxide

Aluminum oxide (alumina; Al_2O_3) has advantages such as its thermal, chemical, and physical properties when compared with several ceramics materials, and is widely used for firebricks, abrasives and integrated circuit (IC) packages. Industrially, more than about 45 million tons of Al_2O_3 are produced in the world, which are mainly manufactured by the Bayer method using bauxite, and about 40 million tons are consumed for refining aluminum[1] Furthermore about 5 million tons of Al_2O_3 are produced as chemical grade and used for various purposes. Moreover about 1.5 million ton Al_2O_3 is used as raw powder in the world. Other Al_2O_3 is consumed for raw powder of aluminum hydroxide, aluminum sulfate and polyaluminum chloride. The amount of Al_2O_3 powder used in Japan is about 350,000 tons, what is about 20% of the total quantity produced in the world. In order to produce Al_2O_3 powder with the quality necessary to be used as ceramic material, various manufacturing methods besides the Bayer method have been developed[1, 2]. Depending on the use of Al_2O_3 in different applications, Al_2O_3 is classified into different grades. Table 1 shows the different soda level requirements in different applications. Commercial grades of Al_2O_3 are often divided into: smelter, calcined (milled or unmilled), low soda, reactive, tabular, activated, catalytic, and high purity. These differ in their particle size, morphology, α-Al_2O_3 content and impurities.

From crystalline structure difference, there are many forms of Al_2O_3 (α, χ, η, δ, κ, θ, γ, ρ). An example of α-phase of Al_2O_3 is corundum/sapphire. The other forms are frequently termed transition Al_2O_3 and arise during the thermal decomposition of aluminum trihydroxides under different conditions. α-Al_2O_3 is the most stable form of the compounds formed between aluminum and oxygen, and is the final product from thermal or dehydroxylation treatments of all the hydroxides. Nomenclatures of the aluminum hydroxides are listed in Table 2[4]

The commonly-used Al_2O_3 is produced through the Bayer process starting from bauxite, which mainly consists of hydrated aluminum. In the Bayer process, crushed bauxite is treated with caustic aluminate solution containing soda. The dissolution reaction is generally carried out under pressure at temperatures ranging from 140 to 280°C. The caustic solution reacts with the aluminum hydroxide so that the impurities can

Table 1: Soda impurity level required for different applications[3]

Normal soda >0.25%	Intermediate soda 0.15–0.25%	Low soda 0.03–0.1%	High pirity thermally reactive
White wares	Electrical porcelain	Spark plugs	Electronic ceramics
Ceramics tile	White ware porcelain	Electronic ceramic component	High density, high strength wear parts
Sanitary ware	Grinding media	Integrated circuit (IC) substrates	Bioceramics
Refractories	Wear tiles	Laboratory wear	Cutting tools
Fused alumina	85–95% alumina components	Wear resistant components	Thin IC substrates
Glass		Zirconia toughened alumina	Armour
Ceramics fibers			

Table 2: Nomenclatures of aluminum hydroxides[4]

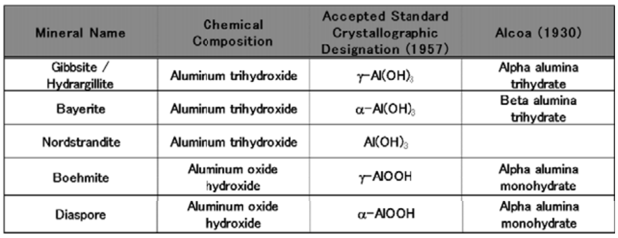

Mineral Name	Chemical Composition	Accepted Standard Crystallographic Designation (1957)	Alcoa (1930)
Gibbsite / Hydrargillite	Aluminum trihydroxide	γ-$Al(OH)_3$	Alpha alumina trihydrate
Bayerite	Aluminum trihydroxide	α-$Al(OH)_3$	Beta alumina trihydrate
Nordstrandite	Aluminum trihydroxide	$Al(OH)_3$	
Boehmite	Aluminum oxide hydroxide	γ-AlOOH	Alpha alumina monohydrate
Diaspore	Aluminum oxide hydroxide	α-AlOOH	Alpha alumina monohydrate

be separated by sedimentation and filtration, leaving a clear solution. After precipitation of the hydroxide, Al_2O_3 powders can be obtained through heat treatment at their transition temperatures.

2. Production Methods of High Purity α-Al_2O_3 Powder

α-Al_2O_3 powders produced by the Bayer method have maximum purity of 99.6-99.9%, which can be used for manufacturing of refractories, spark plugs, and substrates of integrated circuit. The demand of high purity α-Al_2O_3 is increasing for electronic devices, such as YAG (Yttrium-Aluminum-Garnet) and Titanium Sapphire laser devices. High purity α-Al_2O_3 is indispensable in manufacturing substrate of SOS (Silicon on Sapphire) devices, high pressure sodium lamp, and bioceramics[5]. High purity α-Al_2O_3 has also been applied for gas sensors[6]. Because of its stability and strength at high temperature, α-Al_2O_3 is a suitable catalyst material at high temperature or catalyst supports[7]. For those purposes, the purity of α-Al_2O_3 should be higher than 99.99% (4N, four nine).

The manufacturing processes of high purity α-Al_2O_3 by calcinations of starting materials, such as aluminum hydroxide and alum[8], [9], [10], [11] are industrialized. In every process, crystal transformation to α-phase is accompanied by growth of the particles at the time of high temperature calcination of precursor materials such as aluminum trihydroxides and alum[12],[13]. The joints by sintering occur between produced α-Al_2O_3 particles, because transformation to α-Al_2O_3 advances at high temperatures exceeding 1200°C[14],[15]. Consequently, in the manufacturing process of high purity α-Al_2O_3, grinding is necessary to break joints and to control the particle size. Generally, high purity α-Al_2O_3 powders are ground by various grinders such as ball mill, vibration mill and jet mill, in order to obtain mono dispersed particles suitable for sintering[14],[16],[17]. Grinding processes by mechanical techniques to reduce the particle size have been extensively investigated[18)-21]. The influence of grinding on powder characteristics[21], mechano-chemical effects[19],[21] etc., has been reported. Therefore it may be inferred that grinding greatly affects the surface of high purity α-Al_2O_3 powders[22)-26].

High purity α-Al_2O_3 powders are mainly produced by the following methods:

① Hydorlysis of Aluminum Alkoxides

Aluminum alkoxide is obtained from a reaction between metallic aluminum and alcohol groups. Hydrolysis of aluminum alkoxides will produce aluminum hydroxide, which can be transformed after heat treatment into Al_2O_3 powder[8)-10].

The following equations show the reactions of this method, where R is hydrocarbon radical.

$$Al + 3ROH \rightarrow Al(OR)_3 + \frac{3}{2} H_2 \qquad \text{(alkoxide formation)}$$

$$\mathrm{Al(OR)_3 + 3H_2O \rightarrow Al(OH)_3 + 3ROH} \qquad \text{(hydrolysis process)}$$

$$\mathrm{2Al(OH)_3 \rightarrow Al_2O_3 + 3H_2O} \qquad \text{(thermal process)}$$

② Chemical Vapor Deposition

In the conventional chemical vapor deposition (CVD), Al_2O_3 with small particle size is produced by a high temperature reaction at 750-900°C between vaporized $AlCl_3$ and water vapor[27]

$$\mathrm{2AlCl_3 + 3H_2O \rightarrow Al_2O_3 + 6HCl}$$

The volatile $AlCl_3$ is oxidized with oxygen or water vapor at 750-900°C, generating a homogenous particle size of fine Al_2O_3 powder. Processing at temperatures of 750-900°C can produce powders with particle size of 50 nm, consisting of a mixture of γ and α-Al_2O_3. To increase the α-phase content, the powder must be heat-treated at temperatures above 1200°C. Wong et al. reported that formation of dense deposits of α-Al_2O_3 was favored by increasing temperature and decreasing pressure[27] Microstructure of the dense deposits showed long columnar grains[27]

In-situ chemical deposition is a new patented CVD method to produce nearly mono-dispersed single crystal α-Al_2O_3 powder[15],[28] The powder is named as "Sumicorundum" by its manufacturer. The process has the advantage of high crystal growth rate at lower temperature than the conventional method.

③ Thermal Decomposition of Aluminum Alum

Thermal decomposition of ammonium alum method has been used for the manufacturing of kidney jewelry, such as ruby and sapphire. The equation of heat decomposition is shown below.

$$2NH_4Al(SO_4)_2 \cdot 12H_2O \rightarrow Al_2O_3 + 2NH_3 + 4SO_3 + 25H_2$$

The ammonium alum is refined mainly by a recrystallization method, weight decreases in 1/9 by the heat decomposition reaction. Therefore, it is necessary to refine to the purity of ammonium alum one figure higher than the target purity of Al_2O_3. Moreover, it faces the problem about the exclusion processing of the NH_3 and SO_3 gases which occur at the time of heat decomposition[2)]

④ Thermal Decomposition of Inorganic Aluminum Salts

Several inorganic aluminum salts, ammonium aluminum carbonate hydroxide (AACH), $NH_4AlO(OH)HCO_3$, for example, can be heated at 230°C to produce Al_2O_3 through a thermal decomposition shown by the following reaction[11)]

$$2NH_4AlO(OH)HCO_3 \rightarrow Al_2O_3 + 2NH_3 + 2CO_2 + 3H_2O$$

Production condition of AACH will influence the sintering behavior of α-Al_2O_3. The process can generate α-Al_2O_3 powder with purity higher than 99.99% and 0.3-0.4 μm of particle size.

3. Structure of Aluminum Oxide

3.1 Structural Transformations

Beside α-Al_2O_3, there are other forms of metastable Al_2O_3 structures, such as ρ, γ, η, θ, χ and κ-Al_2O_3. Those kinds of transition Al_2O_3 can be produced from heat treatment of aluminum hydroxides or aluminum salts.

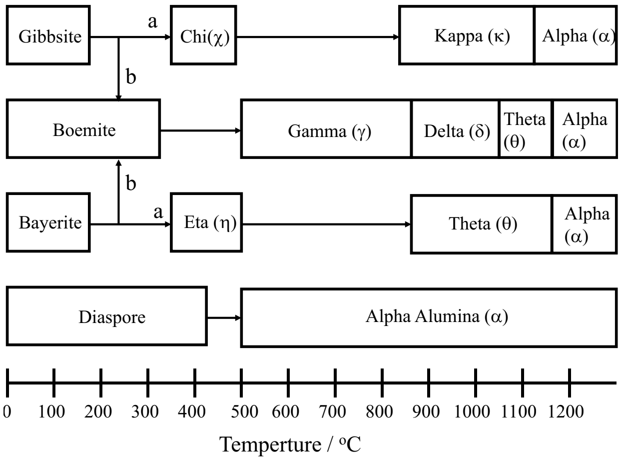

Figure 1: Structure transformation of alumina and aluminum hydroxides[29)]

The aluminum hydroxides can exist in four well-defined forms: the monohydrate AlOOH, as boehmite (γ-monohydrate) and diaspore (α-monohydrate), and the trihydrate $Al(OH)_3$, as gibbsite (γ-trihydrate) and bayerite (α-trihydrate). Of these, all but bayerite occur naturally in bauxite in profound amounts. At high temperatures, all of the heat treatment paths will terminate in α-Al_2O_3. Figure 1 shows the paths of transition Al_2O_3 during the heat treatment processes[29)]

3.2 Crystal Structure of α-Al_2O_3

The crystal structure of α-Al_2O_3, which is called corundum structure, ideally consists of close packed planes (A and B planes) of large oxygen anions (radius 0.14nm) stacked in the sequence[30)] as shown in Figure 2.

The aluminum cations (radius 0.053 nm) have valence of +3 and oxygen anions have valence of –2. There can be only two Al^{3+} ions for every three O^{2-} ions to maintain electrical neutrality. Thus, the cations occupy

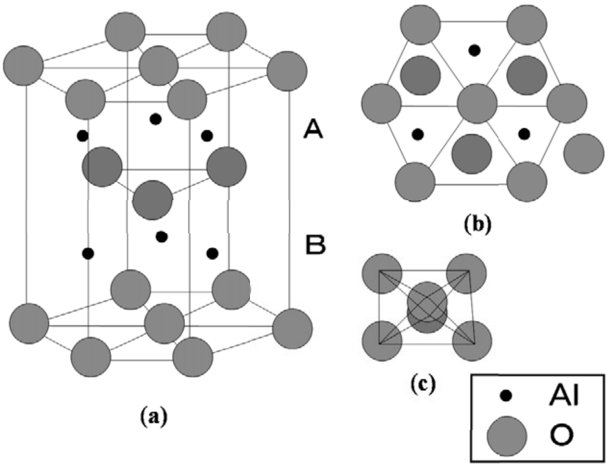

Figure 2: (a) Corundum structure in α-Al_2O_3, (b) top view of the corundum structure, and (c) octahedral structure of α-Al_2O_3[30)]

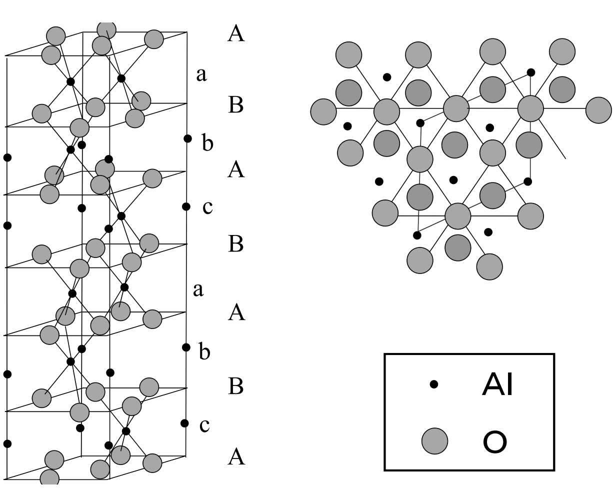

Figure 3: Structure of α-Al_2O_3[32)]

only two-thirds of the octahedral sites of the basic array. This placement forms three different types of aluminum cation layers, named a, b, and c.

In Figure 3, the complete stacking sequence of oxygen and aluminum layers will form A-a-B-b-A-c-B-a-A-b-B-c-A···

One period in this sequence, i.e. from c-A to B-c, forms a hexagonal unit cell of α-Al_2O_3[32)]

3.3 Crystal Structure of Transition Al_2O_3

Transition Al_2O_3 crystallizes in spinel or similar to it with defect lattice. In the spinel structure, the oxygen ions form a face-centered cubic (FCC) lattice and Al^{3+} ions occupy tetrahedral and octahedral interstitial sites, as shown in Figure 4. FCC lattice is also formed by close packed plane, but the stacking sequence is designated as

A-B-C-A-B-C···

Since the Al ion favors octahedral coordination under normal circumstances, Saalfeld et al. assumed all octahedral sites to be occupied, and the cation vacancies being confined to the tetrahedral sites[33)] John et al. used solid-state nuclear magnetic resonance (NMR) with magic angle spinning to determine the coordination of Al ions in the transition Al_2O_3[34)] They found 65 and 75% of the Al ions in the octahedral sites in η and γ-Al_2O_3, respectively. The results on η-Al_2O_3 agree with the X-ray powder diffraction pattern reported by Shirasuka et al.[35)] The cation vacancies, therefore, appear to favor octahedral sites in η-Al_2O_3 but tetrahedral sites in γ-Al_2O_3. The same workers showed that in θ-Al_2O_3 prepared from both bayerite and boehmite, the Al ions were almost exclusively in octahedral coordination. This is in contrast to Saalfeld's[36)] and Yamaguchi et al.[37)] structure analyses of θ-Al_2O_3 in which both assumed half of the Al ions were occupying the tetrahedral sites. Wefer considered the θ structure as an intermediate between the cubic close packing of the low-temperature transition Al_2O_3 and the hexagonally closed-packed corundum[29)]

Ratio of tetrahedral and octahedral sites of Al ions in transition Al_2O_3 still have contradiction between experimental results observed by several researchers. γ-Al_2O_3 has the complex Al-O infrared absorption bands between 350-1100 cm^{-1}, which are interpreted under the criteria for the band assignment of the spinels. The positions of the remainder hydroxyl groups are related with the aluminum vacancies[38)]

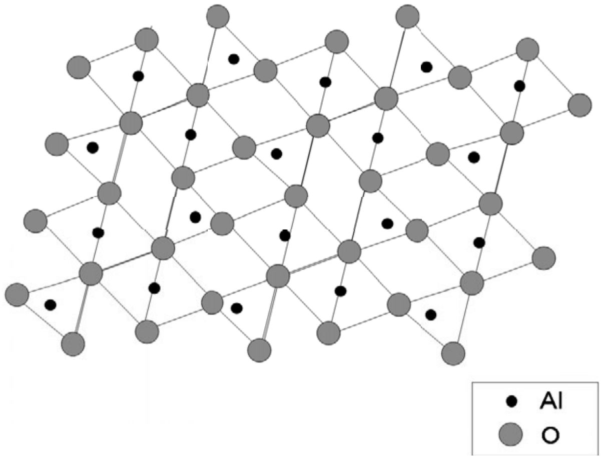

Figure 4: Structure of θ-alumina in which half of the Al ions are occupy tetrahedral sites[32)]

3.4 Crystal Structure of Aluminum Hydroxides

3.4.1 Gibbsite

Pauling first proposed the concept of the gibbsite structure[39)] Double layers of OH ions, with Al ions occupying two-thirds of octahedral interstices within the layers, form the basic structural element. The hydroxyls of adjacent layers are situated, directly opposite to each other, i.e., in a cubic packing. Thus the sequence of OH ions in the direction perpendicular to the planes is A-A-B-B (Figure 5). This superposition of layers and the hexagonal arrangement of Al ions lead to channels through the lattice parallel to the c-axis. Hydrogen bridges OH groups of adjacent double layers. From proton magnetic resonance measurements, Kroon et al. has deduced a model of the spatial distribution of these H-bonds[40)]

3.4.2 Bayerite

Bayerite is rarely found in nature and produced commercially for catalysts or other applications requiring high quality for products. In laboratory, the trihydroxides can be prepared by treatment of aluminum chloride solution with cold ammonium hydroxide, followed by aging at room temperature. According to Fricke et al., bayerite is obtained by hydrolyzing aluminum alcoholates at temperatures below 40°C[41)] Another preparation method is introduced by Torkar et al., who produced extremely pure bayerite electrolytically, using cathode and H_2O_2 as an electrolyte[42)] Bentor et al. reported the first occurrence of the structure verified by X-ray analysis[43)] The structure of bayerite is similar to gibbsite which is built by basic layers of Al-OH octahedra. The layers are, however, arranged in A-B-A-B-A-B sequence (Figure

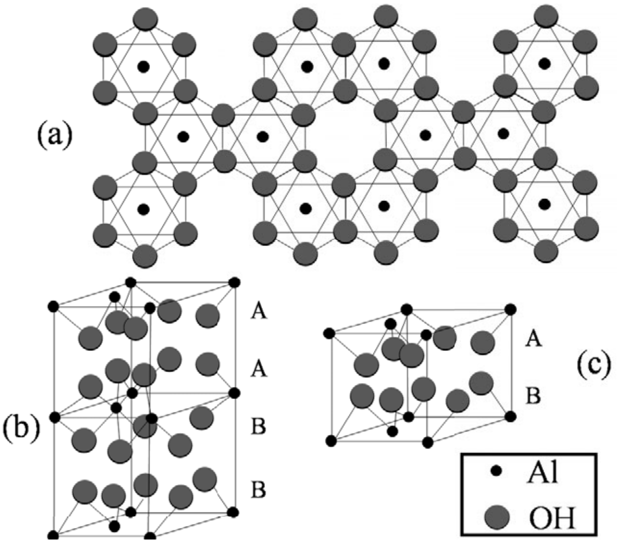

Figure 5: Structure of aluminum trihydroxide; (a) Top view of the gibbsite, (b) gibbsite, and (c) bayerite, respectively. The structures have different layer packing[32]

5)[32]

3.4.3 Nordstrandite

Nordstand et al. published the X-ray difractogram of a trihydroxide which differed from the diffraction patterns of gibbsite and bayerite. They obtained their trihydroxide by precipitating a gel from aluminum chloride or nitrate solutions with ammonium hydroxide[44]

There are two kinds of arrangement for the Al-OH octahedra layer, as shown in Figure 6.

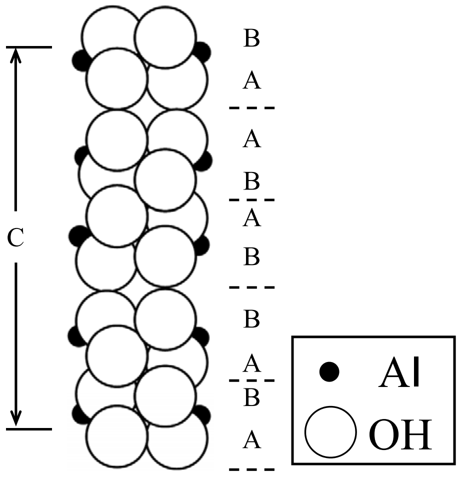

Figure 6: Structure of Nordstrandite[44]

3.4.4 Boehmite

The structure of Boehmite consists of double layers in which oxygen ions are in cubic packing, as shown in Figure 7. These layers are composed of chains formed by double molecules of AlOOH which extend in the direction of the a-axis. The double layers are linked by hydrogen bonds between hydroxyl ions in neighboring planes. Average O-O distance of the hydrogen bridges is 0.27 nm[29] If the excess water is very high (typically contains > 15 wt% excess water), a, b, c distances in 3 dimensional directions of crystallographic dimension become longer, and produce pseudo-boehmite[32] X-ray diffraction pattern of pseudo-boehmite is similar to boehmite with a broad peak. Papee et al. postulated that the excess water is not merely adsorbed on crystallite surface, but is located between boehmite-like layers as molecular water[45] Heating pseudo-boehmite results in the formation of transition Al_2O_3 in a sequence similar to that associated with bayerite[36]

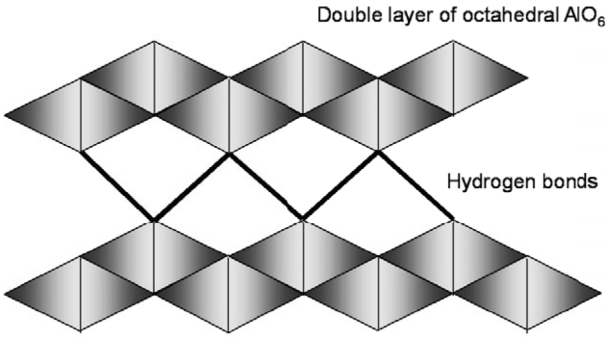

Figure 7: A boehmite structure which consists of double layers and hydrogen bonds in between the layers[32]

4. Reported Al_2O_3 Surfaces

Surface of a solid crystal is regarded as a truncated area of the crystal consisting of coordinately unsaturated site (cus) anions and cations. For this reason, when it is exposed to the atmosphere, all solids become covered with various types of adsorbed species. In the case of metal oxides, the outer layer is usually made up of different adsorbed species. The most abundant component of the surface layer of oxides is water. Besides physisorbed water, absorbed water can be present at the surface in the form of hydrogen bonded or coordinated molecular H_2O, and in a dissociated form as surface hydroxyl[46]

In this regard, infrared spectroscopy has been a commonly used technique to study the surface of Al_2O_3. By infrared spectroscopy, the O-H stretching fundamental vibrations (ν_{OH}) of OH groups located at the surface of oxides can be observed in the high frequency region (wavenumber higher than 2500 cm^{-1}). A very broad band centered at around 3300 cm^{-1} has been assigned to the stretching modes of molecular water hydrogen bonded on an Al_2O_3 surface[47)] and a band at 3500 cm^{-1} to hydrogen bonded hydroxyl groups. At 870 K, the hydrogen bonds no longer exist and only free hydroxyl groups remain[46)]

The knowledge gained so far about the OH band assignments for transition Al_2O_3 is helpful to understand α-Al_2O_3 powders. The vibrational spectrum from the surface hydroxyl of the transition Al_2O_3 is complex and typical. Table 3 tabulates the bands and assignment proposed for surface hydroxyl species on transition Al_2O_3[46)] so far.

Table 3: OH Band assignment proposed for transition aluminas[46)]

OH band	Frequency	Assignment			
		Peri	Tsyganenko	Knozinger	
1	3800	A	I	Ib	Al^{IV}
2	3775	D	I	Ia	□-O-Al^{IV}
3	3745	B	II	IIb	Al^{VI}
4	3730	E	II	IIa	□-O-Al^{VI}
5	3710	C	III	III	bridged
6	3690	C	III	III	bridged
7	3590	H-Bonded		H-bonded	tribridged

Actually the spectra of transition Al_2O_3 consist of a mixture of OH bands that closely overlap with each other. Since transition aluminas are commonly used as catalysts or support of catalyst, their surfaces have been attempted to characterize. Several models have been proposed to explain the reactivity of the surface. Several models as summarized by Morterra are described below[46)]

I: Peri's model (1965)

This model advocates that there are five possible free OH configurations on γ-Al_2O_3 surfaces[48)] These are depicted in Figure 8 and their symbol and frequency are shown also in the third column of Table 3. The major limit of Peri's model consists in the assumption of the (100) crystal face as the only possible termination for aluminas crystallites. This assumption yields an oversimplified picture of the spinel structure, in that only Al^{VI} ions would result present in the uppermost layer and all OH groups in the fully hydrated surface (located on top of equivalent cations) would results to be equivalent. In these conditions, the adoption of random elimination of water from adjoining OH groups is correct and no acidity-basicity concepts associated with different surface OH species needs to be involved. The model is thus valid, in principle, but gives only a partial description of the structurally complex situation of transition aluminas.

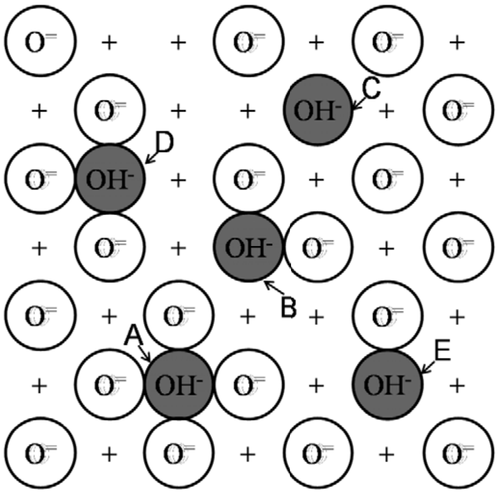

Figure 8: Five types (A-E) of isolated hydroxyl ions (+ denotes Al^{3+} in lower layer). The remaining hydroxyl ions, covering 9.6% of the lattice, are found on five types of sites on which they have from zero to four nearest oxide neighbors, as illustrated and identified[48)]

II: Tsyganenko's model (1973)

By considering the most probable terminations of the crystallites and the geometry of the OH groups in these surface termination groups, Tsyganenko et al. came to the conclusion that the number of nearest neighbors has a negligible effect on the frequency of OH species. The determining factor is the number of lattice metal atoms that the OH groups are attached to.

On the basis of the electronic characteristics of oxygen, there can be three types of OH groups, termed OH groups of type I, II, and III, respectively, depending on the coordination number of the OH group[49)] The three types of hydroxyls are shown in Figure 9.

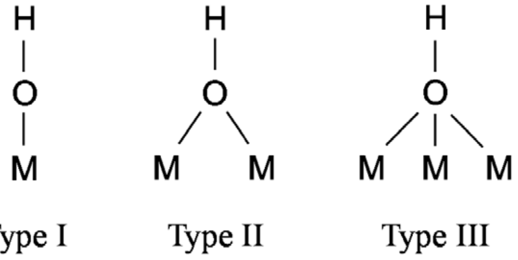

Figure 9: Three types of hydroxyl groups are possible at the surface of transition alumina. M denotes metal ions in a metal oxide[49)]

III: Morterra's model (1976)

Morterra and co-workers considered the coordination of the Al cations, rather than the coordination of the OH group, as the most important factor in determining the OH frequencies[50)-52)] According to their approach, that did not consider the actual crystallographic termination of transition Al_2O_3 and of the other Al-containing systems, the assignment of the various OH species of Al_2O_3 could be made only in very general terms by comparing the OH spectra of different Al oxides. The assignment of OH group is as described in Figure 10.

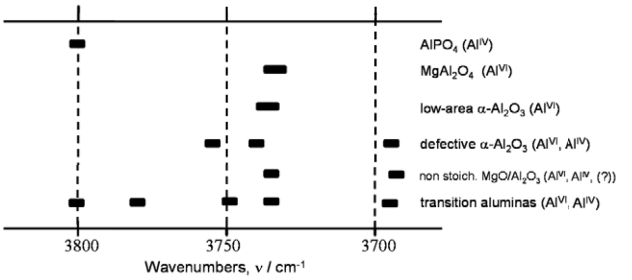

Figure 10: Schematic distribution of OH bands in transition aluminas and other Al-containing oxidic systems[52)]

IV. Knozinger's model (1978)

The OH configurations, frequencies and net charges at Al and OH according to this model are given in Table 4.

The net charge is obtained as the sum of the negative charge of the anion and the sum of the strength of the electrostatic bonds (=cation charge divided by coordination number) to the anion from adjacent cations[53)]

V: The possible role of cation vacancies

The role played by cation vacancies is very difficult to take into account, as there is no way to determine them directly. The possible surface occurrence of cation vacancies is one further parameter, besides OH and cations coordination, that has been considered in the most recent model for OH of aluminas, proposed by Busca et al.[7), 54)] and Della Gata et al.[55)]

As a starting point, Busca's model uses the same general criteria successfully adopted by Knozinger and reported above, but the assignment is also based, on a phenomenological ground, on ;

(i) the observation of the OH spectral patterns of several normal spinels ($MgAl_2O_4$, $ZnAl_2O_4$). Inverse spinels ($NiAl_2O_4$) and defective spinels (transition phase δ-Al_2O_3);

(ii) the spectral characteristics of metal-hydroxy complexes having non-H-bonded OH groups with different coordination numbers.

The conclusions reached, that are schematically reported also in the last column of Table 3, reassign the various OH species of aluminas as reported in Figure 11.

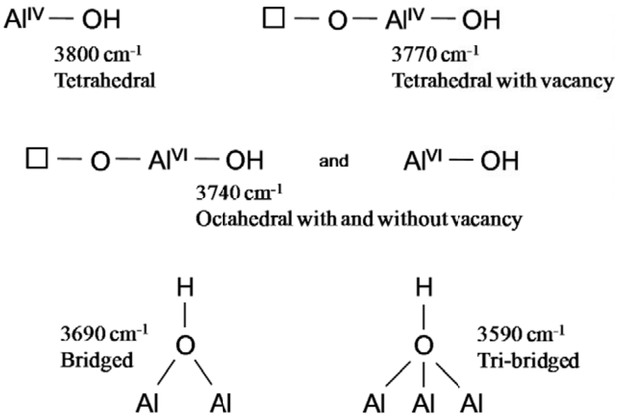

Figure 11: Possible OH stractures, and vOH frequencies, at the surface of defective spinel transition aluminas (Symbol; □ stands for a cation vacancy)[46)]

VI: Morterra's defect model (1994)

Finally, Morterra et al. attributed the 3775 cm^{-1} OH band to hydroxyl group coordinated on tetrahedral Al ion (Al^{IV}-OH groups) present in portions of surface belonging to crystallographically defective configurations (i.e. stepped terminations) which frequently occur in porous system of high surface area and poor crystallinity[56)]

Enormous amount of infrared spectroscopic works have been devoted to understand the surface behavior of Al_2O_3, since Peri proposed a model of Al_2O_3 about thirty years ago. Most of the works have been related to transition Al_2O_3. In spite of some controversial aspects and some remaining uncertainties of the results, the overall picture obtained for the surface properties of the transition Al_2O_3 may be useful for understanding the surface behavior of α-Al_2O_3 in this study.

5. Concluding Remarks

Crystal structural properties, manufacturing methods of high purity Al_2O_3, and surface characteristics on Al_2O_3 oxide powders are described.

The surface chemical characteristics of materials play an important role in many technological processes and applications. Differences in surface conditions of the powders can influence their physical properties such as zeta potential, powder agglomeration and sintering behavior. Ceramics, unlike metals, are mainly produced by sintering, which implies that the surface structure of the raw powder is a controlling factor to determine the final characteristics of sintered ceramics. Control of these behaviors is useful in developing cost effective ceramic powder processing schemes to produce reliable high-performance ceramics with minimal reject rates.

6. Acknowledgement

This research was partially supported by the Ministry of Education, Culture, Sports, Science and Technology (MEXT), Project "Cooperation for Innovative Technology and Advanced Research in Evolution Area". The authors acknowledge Prof. Kozo Ishizaki and Prof. Chanel Ishizaki in Nagaoka University of Technology for helpful advices, discussions and suggestions on this work.

7. References

1) K. Nakano, "Alumina Powders and Their Prices", Ceramics, 36 [4], (2001) 248-253.

2) "2000nen Bihunmatusizyouno Genzyouto Syouraitenbou", Fujikimerasouken, (2000) pp. 69-74.

3) K. A. Evans, "The Manufacture of Alumina and its Use in Ceramics and Related Applications", Key Eng. Mater., 489, (1996) 122-124.

4) K. Wefers and C. Misra, "Oxides and Hydroxides of Aluminum", Alcoa Laboratories, Aluminum Company of America, Pittsburgh, (1987) p.2.

5) Yogyo Kyokai Hensyuiinkai, "Ceramic Processing", Gihodo, Tokyo, (1993) p. 105.

6) W. Gopel, J. Hesse and J. N. Zemel, "Sensors -A Comprehensive Survey-", Vol. 7, Chemical Sensors, Verlag Chemie, Wienheim, (1990).

7) G. Busca, V. Lorenzelli, V. S. Escribano and R. Guidetti, "FT-IR Study of the Surface Properties of the Spinels $NiAl_2O_4$ and $CoAl_2O_4$ in Relation to Those of Transitional Aluminas", J. Catal., 131, (1991) 167-177.

8) B. E. Yoldas, "Hydrolysis of Aluminum Alkoxides and Bayerite Conversion", J. Appl. Chem. Biotech., 23, (1973) 803-809.

9) H. Endl, B. D. Kruse and H. Hausner, "Effects of Processing Parameters in the Preparation of Ultrapure Aluminum Oxide from Aluminum Isopropylate", Berichte der Deutschen Keramischen Gesellschaft, 54 [4], (1977) 105-110.

10) H. Kadokura, H. Umezaki and Y. Higuchi, "Process for Producing High Purity Metallic Compound", US. Patent, No. 4, 650, 895, (1987).

11) S. Kato, T. Iga, S. Hatano, and Y. Isawa, "Effects of Synthetic Conditions of $NH_4AlO(OH)HCO_3$ on Sinterability of Alumina Obtained by Thermal Decomposition", Yogyo Kyokai Shi, 84 [6], (1976) 255-258.

12) S. Iijima, "Ultra-Fine Spherical Particles of γ-Alumina: Electron Microscopy of Crystal Structure and Surface Morphology at Atomic Resolution", Jpn. J. Appl. Phys., 23 [6], (1984) 347-350.

13) Y. Takeuchi, H. Umezaki and H. Kadokura, "High Puriy Alumina Derived from Aluminum Alkoxide", Sumitomokagaku, 1993-I, (1993) 4-14.

14) Y. Takeuchi, H. Umezaki and H. Kadokura, "High Puriy Alumina Derived from Aluminum Alkoxide", Sumitomokagaku, 1993-I, (1993) 4-14.

15) M. Mouri, S. Tanaka, Y. Uchida and Y. Sawabe, "Development of Advanced Alumina "SUMICORUNDUM"", Sumitomokagaku, 1996-II, (1996) 4-14.

16) H. Umezaki, Y. Takeuchi and H. Takahashi, "Toukousei Alumina Genryou Hunmatsuno Seizouhou", J.P Patent, No. H4-108545, (1992).

17) K. Yamamoto and Y. Takeuchi, "Alumina Hhunmatsuno Seizouhouhou", J.P Patent, No. P2001-302233A, (2001).

18) K. Tanaka, K. Minai, K. Wakino and I. Uei, "Submicron Grinding of $BaTiO_3$ by Ball Milling", J. Soc. Mater. Sci. Jpn., 35 (1986) 54-58.

19) K. Tanaka, I. Inada, K. Wakino and I. Uei, "Submicron Grinding of Low-soda Alumina by Ball Milling", J. Soc. Mater. Sci. Jpn., 37 (1987) 1319-1325.

20) Y. Kondo, Y. Hashizuka, M. Nakahara, K. Yokota and K. Ishizaki, "Influence of Combination of Ball Diameters and Rotation Speed on Grinding Performance of Alumina by Ball Milling", J. Ceram. Soc. Jpn., 101 [7], (1996) 819-823.

21) K. Yokota, Y. Hashizuka, M. Nakahara and Y. Kondo, "Characteristics of the Ground Alumina Powders by Wet Rotation Ball Milling", J. Ceram. Soc. Jpn., 103 [11], (1995) 1167-1171.

22) T. Shirai, Ch. Ishizaki and K. Ishizaki, "Effect of Manufacture Process on Water Surface Adsorption of High Purity α-Al_2O_3 Powders", Interceram, 50, 3, (2001) 176-181.

23) T. Shirai, K. Matsumaru, Ch. Ishizaki and K. Ishizaki, "Analysis of Hydration and Adsorption Layer on Commercial Sub-micron High Purity α-alumina Powders", J. Japan Inst. Metals , 68, 2, (2004) 102-105.

24) T. Shirai, J. W. Li, K. Matsumaru, C. Ishizaki and K. Ishizaki, "Surface Hydration States of Commercial High Purity α-Al_2O_3 Powders Evaluated by Temperature Programmed Desorption Mass Spectrometry and Diffuse Reflectance Infrared Fourier Transform Spectroscopy",

Sci. and Tech.of Adv. Mat., 6 [2] (2005) 123-128.

25) T. Shirai, C. Ishizaki and K. Ishizaki, “Effects of Manufacturing Processes on Hydration Ability of High Purity α-Al$_2$O$_3$ Powders”, J. Ceram. Soc. Japan, 114 [3] (2006) 286-289.

26) T. Shirai, C. Ishizaki and K. Ishizaki, “Tetrahedral Aluminum Ions on High Purity Sub-micron α-alumina Powder Surfaces”, J. Ceram. Soc. Japan, 114 [5] (2006) 415-417.

27) P. Wong and M. Robinson, “Chemical Vapor Deposition of Polycrystalline Alumina”, J. Am. Ceram. Soc., 53 [11], (1970) 617-621.

28) Y. Uchida, Y. Sawabe, M. Mohri, N. Shiraga and Y. Matsui, ”Nearly Monodispersed Single Crystal Particles of □-alumina”, Science, Technology and applications of colloidal suspensions, (1995) 159-165.

29) K. Wefers and C. Misra, “Oxides and Hydroxides of Aluminum”, Alcoa Laboratories, Aluminum Company of America, Pittsburgh, (1987) p. 47.

30) Y. Kim and T. Hsu, “A Reflection Electron Microscopic (REM) Study of α-Al$_2$O$_3$ (0001) Surfaces”, Surface Science, 258, (1991) 131-146.

31) W. F. Smith, “Foundation of Materials Science and Engineering”, 2nd edition, McGraw-Hill, Singapore, (1993) p.530.

32) G. Yamaguchi, “Arumina to Aruminasuiwabutsu no Kouzou”, Kagaku to Kougyou, 17 [12], (1964) 1326-1335.

33) H. Saalfeld and B. Mehrotra, “Electron-Diffraction Study of Aluminum Oxides”, Berichte der Deutschen Keramischen Gesellschaft, 42, (1965) 161-166.

34) C. S. John, V. C. M. Alma and G. R. Hays, “Characterization of Transition Alumina by Solid-State Magic Angle Spinning Aluminum NMR”, Applied Catalysis, 6, (1983) 341-46.

35) H. Shirasuka, H. Yanagida and G. Yamaguchi, “The Preparation of η Alumina and its Structure”, Yogyo Kyokai Shi, 84 [12], (1976) 610-613.

36) H. Saalfeld, “The Structures of Gibbsite and of the Intermediate Products of its Dehydration”, Neues Jahrb. Mineral. Abhandl., 95, (1960) 1-87.

37) G. Yamaguchi, I. Yasui and W. C. Chiu, “A New Method of Preparing θ-Alumina and the Interpretation of its X-ray Powder Diffraction Pattern and Electron Diffraction Pattern”, Bull. Chem. Soc. Jap., 43, (1970) 2487-2491.

38) J. M. Saniger, “Al-O Infrared Vibrational Frequencies of γ-alumina”, Mater. Lett., 22, (1995) 109-113.

39) L. Pauling, “The Structure of the Micas and Related Minerals”, National Academy of Sciences USA Proceedings, National Academy of Sciences USA, 16, (1930) 123-128.

40) D. J. Kroon and C. Stople, “Position of Protons in Aluminum Hydroxides Derived from Proton Magnetic Resonance”, Nature, 183, (1959) 944-45.

41) R. Fricke and K. Jockers, “Simple Preparation of Boehmite”, Z. Naturforsch, 26, (1947) 244.

42) K. Torkar and O. Bergmann, “Aluminum Hydroxides and Oxides. I. Preparation of Extremely Pure Aluminum Hydroxides by Electrolysis”, Monatsh. Chem., 91, (1960) 400-405.

43) Y. K. Bentor, H. Gross and L. Heller, “Some Unusual Minerals from the “Mottled Zone” Complex, Israel”, Ame. Minera., 48, (1963) 924-930.

44) R. A. V. Nordstrand, W. P. Hettinger and C. D. Keith, “”Nature, 177 (1956)713-714.

45) D. Papee, R. Tertain and R. Biais, “Constitutions of Gels and Crystalline Hydrates of Alumina”, Bulletin de la Societe Chimique de France, (1958) 1302-1310.

46) C. Morterra and G. Magnacca, “A Case Study: Surface Chemistry and Surface Structure of Catalytic Aluminas, as Studied by Vibrational Spectroscopy of Adsorbed Species”, Catalysis Today, 27, (1996) 497-532.

47) M. I. Baraton, “FT-IR Surface Study of Nanosized Ceramic Materials Used as Gas Sensors”, Sensor and Actuators B, 31, (1996) 33-38.

48) J. B. Peri, “A Model for the Surface of γ-Alumina”, J. Phys. Chem., 69, (1965) 220-230.

49) A. A. Tsyganenko and V. N. Filimonov, “Infrared Spectra of Surface Hydroxyl Groups and Crystalline Structure of Oxides”, J. Mole. Str., 19, (1973) 579-589.

50) C. Morterra, G. Ghiotti, E. Garrone and F. Boccuzzi, “Infrared Spectroscopic Characterization of α-Alumina Surface”, J. Chem. Soc., 1 [72], (1976) 2722-2734.

51) C. Morterra, G. Ghiotti, F. Boccuzzi and S. Coluccia, “An Infrared Spectroscopy Investigation of the Surface Properties of Magnesium Aluminate Spinel”, J. Catal., 51, (1978) 299-313.

52) Z. Zecchina, S. Coluccia and C. Morterra, “Infrared Spectra of Molecules Adsorbed on Oxide Surfaces”, Appl. Spect. Rev., 21, (1985) 259-310.

53) H. Knozinger and P. Ratnasamy, “Catalytic Aluminas: Surface Models and Characterization of Surface Sites”, Catal. Rev., Sci. Eng., 17, (1978) 31-70.

54) G. Busca, V. Lorenzelli, G. Ramis and R. J. Willey, “Surface Sites on Spinel-Type and Corundum-Type Metal Oxide Powders”, Langmuir, 9, (1993) 1492-1499.

55) G. Della Gatta, B. Fubini, G. Ghiotti, C. Morterra, “The Chemisorption of carbon Monoxide on Various transition Aluminas”, J. Catal., 43, (1976) 90-98.

56) C. Morterra, V. Bolis and G. Magnacca, “IR Spectroscopic and Microcalorimetric Characterization of Lewis Acid Sites on (Transition Phase) Al2O3 Using Adsorbed CO”, Langmuir, 10, (1994) 1812-1824.